ARTICLES

Simulations of Gas-Phase Chemical Reactions: Applications to S_N2 Nucleophilic Substitution

William L. Hase

Computer simulations and animations of the motion of atoms as a chemical reaction proceeds give a detailed picture of how the reaction occurs at a microscopic level. This information is particularly useful for testing the accuracy of statistical models, which are used to calculate various attributes of chemical reactions. Such simulations and animations, in concert with experimental and ab initio studies, have begun to provide a microscopic picture of the intimate details of a particular class of gas-phase ion-molecule bimolecular reactions known as S_N2 nucleophilic substitution. In these reactions, a nucleophile is displaced from a molecule by another nucleophile. The dynamical model of S_N2 reactions that emerges from the computer studies, and its relation to statistical theories, is discussed here.

A complete understanding of a chemical reaction requires knowing how it occurs at an atomic or microscopic level (*1*, *2*). A picture of a chemical reaction's microscopic dynamics would reveal how energy flows and atoms move as reactants proceed to products. A bimolecular reaction, such as A + BC → AB + C, can either occur directly or can proceed through an ABC collision intermediate that has a detectable lifetime. For a unimolecular reaction, such as ABC → AB + C, it is important to understand the dynamics of energy flow between the ABC vibrational modes before dissociation occurs (*3*). This energy flow is often called intramolecular vibrational energy redistribution (*4*).

Another important reason for studying microscopic reaction dynamics is to determine the accuracy of various theoretical models, which are based on statistical assumptions and are used to calculate reaction rates and the partitioning of available energy to the reaction products. Two widely used theories for calculating reaction rates are transition-state theory (TST) and Rice-Ramsperger-Kassel-Marcus (RRKM) theory (*5*, *6*).

Statistical Theories

The TST is used to calculate thermal rate constants for both bimolecular and unimolecular reactions when there is a free-energy barrier (*7*–*10*) separating the reactants and products. This barrier defines the transition state. The assumption of TST is that a trajectory crossing this barrier, on its way from reactants to products, does not recross and return to reactants (*10*). TST is often called a statistical theory because the TST rate constant is proportional to a statistical thermodynamic partition function for the transition state.

The RRKM theory is used to calculate unimolecular rate constants versus total energy. A statistical assumption of RRKM theory is that energy flow (that is, intramolecular vibrational energy redistribution) between the unimolecular reactant's vibrational modes is unrestricted and complete on the time scale of the unimolecular reaction (*11*). A transition state, which separates reactants from products, is assumed in RRKM theory and, according to variational RRKM theory (*12*–*14*), is placed at the minimum in the sum of states for the degrees of freedom orthogonal to the reaction coordinate as the system moves along the reaction path. If the unimolecular reaction has a well-defined potential energy barrier, this variational criterion typically places the transition state at or near this point. As in TST theory, RRKM theory assumes no recrossing of the transition state.

The RRKM theory assumes that energy is distributed statistically between vibrational modes at the transition state. If additional assumptions are made regarding the coupling of vibrational modes in moving from the transition state to products, vibrational, rotational, and translational energy distributions can then be calculated for the products (*15*–*19*). In orbiting transition state–phase space theory (OTS-PST), orbital angular momentum is assumed to remain conserved in moving from an orbiting transition state to products (*15*, *16*, *18*).

Although statistical theories like TST, RRKM, and OTS-PST are widely used to interpret experiments, one usually does not know whether the fundamental assumptions of these theories are correct. This issue is further complicated by a lack of understanding about the consequences of the failure of these assumptions. Studies of the microscopic dynamics of chemical reactions provide the detailed information needed to test the fundamental assumptions of statistical theories.

Viewing Microscopic Reaction Dynamics

There are numerous experimental approaches to finding clues about the microscopic properties of a chemical reaction (*1*, *2*). The reaction path and time scale for a bimolecular reaction can be investigated by measuring the energy and scattering angle distributions of the products and determining the dependence of the reaction probability on the orientation and mode-specific excitation of the reactants. The microscopic dynamics of a unimolecular reaction can be probed by measuring the rate constant and product energies for different selective excitations of the unimolecular reactant. A direct experimental observation of both bimolecular and unimolecular microscopic dynamics can be made by real-time laser femtochemistry (*20*, *21*), in which motions of the atoms involved in the reaction are observed.

A complementary approach to these experimental studies is to use dynamical calculations, performed on a high-speed computer, to simulate the motion of the atoms as the reaction proceeds (*22*). Besides giving a complete picture of the reaction event, such calculations often provide further insight into the experimental observations and can be used to test theories such as TST and RRKM theory. It is possible to carry out quantum dynamical calculations for chemical reactions of three or four atoms, such as $F + H_2 \rightarrow HF + H$ or $H_2 + OH \rightarrow H_2O + H$ (*23*–*26*); however, for larger reactive systems, such calculations are extremely time-consuming. Although classical trajectory (molecular dynamics) calculations have well-understood limitations (*27*, *28*), they have proven valuable for polyatomic reactive systems and are very good for visualizing atomic motions.

A standard procedure for performing a classical trajectory simulation is to numerically integrate Hamilton's equations of motion (*29*)

$$\dot{q}_i = \partial H/\partial p_i \qquad \dot{p}_i = -\partial H/\partial q_i \qquad (1)$$

where H, the Hamiltonian, is the sum of the kinetic and potential energies and the dot denotes a derivative with respect to time. Values for the coordinates q_i and momenta p_i are selected randomly by Monte

---

The author is with the Department of Chemistry, Wayne State University, Detroit, MI 48202, USA.

Carlo methods from distribution functions that represent the properties of the reactants. The trajectory starts at these initial values of q_i and p_i and is then followed in time to determine its outcome. To determine statistically meaningful average values and distributions for final properties, it is usually necessary to calculate a large number of trajectories (for example, 100 to 1000).

A trajectory gives the coordinates of the atoms throughout time. If only a small number of atoms (two or three) are critically involved in the reaction event, the microscope dynamics can often be depicted by plots of internuclear coordinates versus time. However, if the chemical process is a polyatomic event that involves many atoms, correlations between internuclear coordinates become important. A powerful way to visualize these correlations and obtain a microscopic picture of the chemical event is by computer animation of the atomic motions determined from the simulation of the classical trajectory.

S_N2 Reactions and Statistical Theories

A class of chemical reactions for which there has been an exceptional synthesis of experimental (*30–43*), ab initio (*44–52*), quantum and semiclassical dynamical (*53–56*), and trajectory simulation and animation (*57–62*) studies of microscopic dynamics are gas-phase bimolecular nucleophilic substitutions (*63*), or S_N2 reactions of the type

$$X^- + RY \rightarrow XR + Y^- \qquad (2)$$

where X and Y are halogen atoms. In the symbol S_N2, S stands for substitution, N for nucleophilic, and 2 for bimolecular. The computer simulations and animations have been of tantamount importance in the depiction of the fundamental microscopic dynamics of these reactions. Significant deviations from the assumptions of statistical theories have been observed, and insight has been acquired for the development of an accurate theoretical model.

Pioneering experimental studies (*30–33*) and quantum chemical calculations (*44–48*) have shown that the reaction path potentials for gas-phase S_N2 reactions have double wells separated by a central barrier. The double wells arise from the $X^-\cdots RY$ and $XR\cdots Y^-$ ion-molecule complexes, whose principal interaction potential is that between a charge and a dipole. Reaction path potentials for the $Cl^- + CH_3Cl$ and $Cl^- + CH_3Br$ S_N2 reactions are illustrated in Fig. 1. The asymmetric $Cl^- + CH_3Br$ reaction is exothermic, and the $ClCH_3\cdots Br^-$ complex in the exit channel is at a lower energy than the $Cl^-\cdots CH_3Br$ complex in the entrance channel. For the symmetric $Cl^- + CH_3Cl$ reaction, the central barrier is higher than the potential of the asymptotic limits, but there are other symmetric systems, such as $Cl^- + ClCH_2CN$ (*40*), for which the central barrier is lower. The central barrier for $Cl^- + CH_3Br$ is lower than the reactant potential (*37*), and it is a general property of S_N2 reactions that the height of the central barrier, relative to the reactant potential, decreases as the exothermicity of the reaction increases (*63*). For the highly exothermic reaction $F^- + CH_3Cl$, the central barrier is only ~3 kcal/mol higher than the potential energy minimum of the $F^-\cdots CH_3Cl$ complex (*64*).

Many of the initial investigators (*30–34*) of S_N2 nucleophilic substitution measured reaction rates and analyzed them using theoretical models such as TST and RRKM theory. For a S_N2 reaction like $Cl^- + CH_3Cl$, which has a central barrier higher than the reactant asymptotic limit, crossing the central barrier is rate determining according to TST. Thus, TST predicts the S_N2 rate constant to be

$$k_{S_N2} = \frac{k_B T}{h} \exp(-\Delta G^{\ddagger}/RT) \qquad (3)$$

where k_B is Boltzmann's constant, T is temperature, h is Planck's constant, $\Delta G^{\ddagger}$ is the difference in free energy between the central barrier and the reactants, and R is the gas constant. If recrossings of the central barrier are unimportant, TST is valid for the S_N2 reaction regardless of the nature of the molecular dynamics in other regions of the potential energy surface.

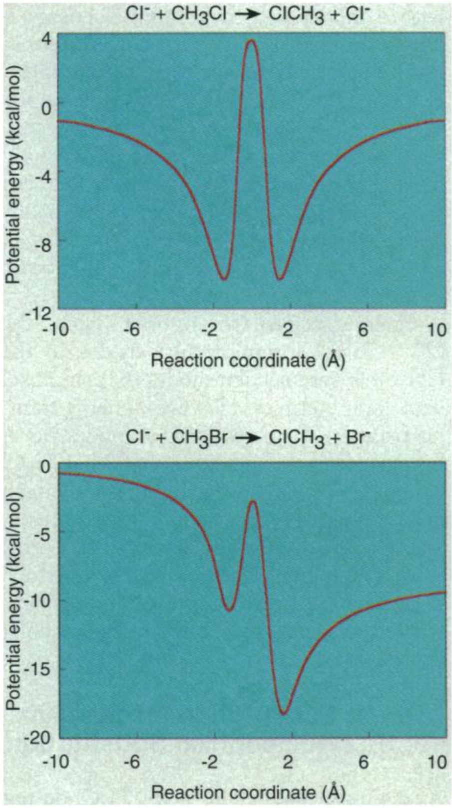

Fig. 1. Reaction path potentials for $Cl^- + CH_3Cl \rightarrow ClCH_3 + Cl^-$ and $Cl^- + CH_3Br \rightarrow ClCH_3 + Br^-$ S_N2 nucleophilic substitution.

For highly exothermic S_N2 reactions, which have a central barrier significantly lower in energy than that of the reactants, TST assumes that association of the reactants is the rate-controlling step (*35*). The S_N2 rate constant can then be modeled by a capture theory (*65*) such as variational TST (*9, 10, 66*), average dipole orientation theory (*67*), or the theory of classical trajectories (*66, 68*).

RRKM theory has been used to model the S_N2 rate constant (*31–34, 40*) when, according to TST, neither central barrier crossing nor reactant association is rate determining. RRKM theory assumes that for every species crossing the entrance-channel variational transition state, vibrational energy becomes completely randomized so that the subsequent dynamics of the species can be modeled as that of an equilibrated microcanonical ensemble. If RRKM theory predicts $XR\cdots Y^- \rightarrow XR + Y^-$ dissociation to be much faster than $XR\cdots Y^- \rightarrow X^-\cdots RY$ isomerization (which is the case for the $ClCH_3\cdots Br^-$ complex in Fig. 1), the S_N2 rate constant is expressed as the following integral over energy and angular momentum

$$k_{S_N2} = \iint \frac{k_{as}(E,J)k_{isom}(E,J)P(E)P(J)dEdJ}{k_{isom}(E,J) + k_{dis}(E,J)} \qquad (4)$$

where $P(E)$ and $P(J)$ are the energy and angular momentum probability distributions, $k_{as}(E,J)$ is the variational TST rate constant for $X^- + RY$ association, and $k_{isom}(E,J)$ and $k_{dis}(E,J)$ are the isomerization and dissociation RRKM rate constants for the $X^-\cdots RY$ complex.

Although the energetics, transition states, and rates of S_N2 reactions are important, they do not provide a complete picture of the microscopic reaction dynamics. There are several basic questions associated with the microscopic dynamics of gas-phase S_N2 nucleophilic substitution that are important to the development of accurate theoretical models for bimolecular and unimolecular reactions. Collisional association of X^- with RY (that is, reaction 2) to form the $X^-\cdots RY$ complex requires energy transfer from relative translational motion to vibrational or rotational, or both, degrees of freedom of RY. Understanding the dynamics of this process is a fundamental problem in ion-molecule chemistry. It has been proposed (*30–33*) that during the course of a S_N2 reaction, the system becomes trapped in the $X^-\cdots RY$ and $XR\cdots Y^-$ complexes. The interaction between the ion and molecule in these complexes is weak, similar to the intermolecular interactions for a van der Waals molecule, and there is considerable interest in the intramolecular and unimolecular dynamics of such weakly coupled systems (*69*). Reaction 2 is akin to the generic displacement reaction A + BC → AB + C, and as for all displacement reactions of this type, there is considerable interest as to whether its rate can be enhanced by selective vibrational excitation of RY (*70–73*). Finally, the dynamics of crossing the S_N2 central barrier with the additional possibility of recrossings is a central issue in reaction rate theory (*10*). In the sections below, experimental, computer simulation, and animation studies of these questions of dynamics and their relation to statistical theories are reviewed.

Formation and Lifetime of the $X^-\cdots RY$ Complex

To form the $X^-\cdots RY$ complex during a $X^- + RY$ collision, the relative translational energy of $X^- + RY$ must be transferred to either RY rotation or vibration; otherwise the reactants will simply rebound without forming the complex. In a trajectory simulation of $Cl^- + CH_3Cl$ collisions (*61*), it was found that the $Cl^-\cdots CH_3Cl$ complex is formed by a translation to rotation (T → R) energy transfer process, which involves coupling between the orbital angular momentum of the reactants and the rotational angular momentum of CH_3Cl. Complex formation does not involve energy transfer to CH_3Cl vibration. Thus, energy is initially stored only in the three low-frequency intermolecular modes of the $Cl^-\cdots CH_3Cl$ complex (that is, the $Cl^-\cdots C$ stretch and degenerate bending modes). This initially prepared complex is called an intermolecular complex (*60*) because only the intermolecular modes are excited.

The energy transfer mechanism for complex formation can easily be determined from the trajectories by calculating the CH_3Cl internal energy as a function of time. Initially, the internal energy is only rotational, and transfer of this energy to CH_3Cl vibration (R → V) occurs on a much longer time scale. The mechanism for complex formation is visualized from the computer animations by observing which orientations between the reactants lead to complex formation (*61*). For this formation to occur by T → R, the reactants must sample the anisotropic part of the interaction potential. Collisions with a $Cl^-\cdots C\text{–}Cl$ angle of approximately π, with the CH_3Cl dipole oriented, do not form the $Cl^-\cdots CH_3Cl$ complex. Collisions oriented in this manner could yield complexes by T → V, but this is an unimportant energy transfer mechanism (*61*). Both R → V and T → V energy transfer processes are unimportant because the frequencies associated with the rotation of CH_3Cl relative to Cl^- and with the $Cl^- + CH_3Cl$ relative translation are much lower than the intramolecular frequencies of the CH_3Cl moiety. When there is such a mismatch in frequencies, energy transfer may be very inefficient (*3*).

Because oriented collisions do not lead to complex formation, the $Cl^- + CH_3Cl \rightarrow Cl^-\cdots CH_3Cl$ rate constant calculated from the trajectories is less than that given by a capture model (*65*). Experimental support for this result comes from studies (*35, 36*) of highly exothermic S_N2 reactions such as F^- with CH_3Cl, CH_3Br, and CH_3I; for these reactions, the central barrier is expected to be too low to influence the reaction rate, so that the rate is controlled by association of the reactants. For a relative translational energy of 1 eV, the reaction rate constants for $F^- + CH_3Cl$ and $F^- + CH_3I$ are one-tenth and one-fourth of the capture rate constant, respectively (*35*).

The unimolecular dynamics of the $Cl^-\cdots CH_3Cl$ complexes are studied from the trajectories by calculating the relative number of complexes that stay intact over time (*58, 59*) and the rate at which energy is transferred to the CH_3Cl intramolecular vibrational modes (*61*). The predominant process for the $Cl^-\cdots CH_3Cl$ complex is dissociation back to the reactants $Cl^- + CH_3Cl$, with a rate constant consistent with a model in which internal energy is only transferred between the three intermolecular modes of the complex. For complexes formed by $Cl^- + CH_3Cl$ collisions at 300 K, the unimolecular dissociation rate constant has been found to be about 0.1 ps^{-1} from both trajectories (*59*) and experiment (*74*). If energy were transferred statistically between all of the vibrational modes of $Cl^-\cdots CH_3Cl$, the rate constant would be an order of magnitude smaller.

Energy begins to transfer from the $Cl^-\cdots CH_3Cl$ intermolecular modes to the CH_3Cl intramolecular modes for complexes with long lifetimes. However, energy transfer between these two sets of modes never becomes facile. The number of $Cl^-\cdots CH_3Cl$ complexes with long lifetimes is much greater than that predicted by RRKM theory (*6*), which assumes unrestricted energy flow. These long-lived complexes, in which energy has been transferred to the intramolecular modes, are called intramolecular complexes (*60*).

Direct Substitution Mechanism for S_N2 Nucleophilic Substitution

As discussed above, Cl^- and CH_3Cl do not associate under thermal conditions when the CH_3Cl dipole is oriented with a $Cl^-\cdots C\text{–}Cl$ angle of approximately π. Because these oriented trajectories follow the reaction path, it is of interest to determine whether they can be modified to promote S_N2 nucleophilic substitution. What was discovered from the trajectory simulations and animations (*59, 61*) was that the addition of three or more quanta to the C–Cl stretch mode of the CH_3Cl reactant opens up a direct substitution mechanism without trapping in either of the potential energy wells. This direct reaction only occurs for oriented collisions with a collision angle $\theta \approx \pi$, so that the value of θ as the reactants interact, the dynamical stereochemistry (*75*), can be used to distinguish between the association and direct substitution mechanisms.

Both a direct substitution trajectory and a complex-forming trajectory are depicted on the contour diagrams of Fig. 2. For each trajectory there is initially six quanta in the C–Cl stretch mode. Adding quanta to the C–Cl bond promotes bond extension, so that the central barrier can be reached as Cl^- approaches. This dynamical effect is in accord with the role of vibrational energy in A + BC → AB + C triatomic displacement reactions (*73*).

The importance of this direct substitution mechanism is strongly dependent on the rotational energy of CH_3Cl. If CH_3Cl has no rotational energy, most of the collisions have dipole orientation and direct substitution is important. For $Cl^- + CH_3Cl$ trajectories with a relative translational energy corresponding to 300 K (that is, $3RT/2$), no CH_3Cl rotational energy, and six quanta in the C–Cl vibrational mode, direct substitution is about two times more probable than association (*61*). However, by simply increasing the CH_3Cl rotational temperature to 300 K, one can make the direct substitution/association ratio less than 0.06.

For the $Cl^- + CH_3Cl$ system, direct substitution only occurs when the C–Cl stretch normal mode is excited with three or more quanta. For CH_3Cl at 300 K, the probability of this vibrational excitation and rate constant with vibrational excitation is too small to make direct substitution an important contributor to the $Cl^- + CH_3Cl \rightarrow ClCH_3 + Cl^-$ S_N2 nucleophilic substitution. However, the direct substitution mechanism may become more important if less vibrational excitation is needed to promote it. This may be the case for $Cl^- + CH_3Br$ and $F^- + CH_3Cl$, which have a lower central barrier than the $Cl^- + CH_3Cl$ reaction (*37, 62, 64*).

Dynamical Model for Association and Substitution

A dynamical model for S_N2 nucleophilic substitution that emerges from the trajectory simulation and animation studies for the $Cl^- + CH_3Cl$ system is depicted in Fig. 3.

The complex formed by a collision between the reactants is an intermolecular complex $C_{\mathrm{inter,R}}$. To cross the central barrier, this complex has to undergo a unimolecular transition in which energy is transferred from the intermolecular modes to the CH_3Cl intramolecular modes, which forms the intramolecular complex $C_{\mathrm{intra,R}}$. The $C_{\mathrm{inter,R}} \rightarrow C_{\mathrm{intra,R}}$ rate does not involve the crossing of a potential energy barrier but results from a dynamical barrier for energy transfer (3). The intramolecular complex accesses the central barrier region of the potential energy surface and $Cl^- \cdots CH_3Cl \rightarrow ClCH_3 \cdots Cl^-$ isomerization occurs by a $C_{\mathrm{intra,R}} \rightarrow C_{\mathrm{intra,P}}$ transition. Products are formed when $C_{\mathrm{intra,P}} \rightarrow C_{\mathrm{inter,P}}$ occurs.

The scope of the dynamical model in Fig. 3 is unknown, but it appears to also be applicable to $Cl^- + CH_3Br \rightarrow ClCH_3 + Br^-$ S_N2 nucleophilic substitution. Both trajectories (62) and experiments (43) have examined the intramolecular and unimolecular dynamics of the $Cl^- \cdots CH_3Br$ complex. When the complex's low-frequency intermolecular modes are excited in the trajectory simulations (62), it preferentially dissociates to $Cl^- + CH_3Br$. However, this becomes a negligible reaction path, and instead, $Cl^- \cdots CH_3Br \rightarrow ClCH_3 \cdots Br^-$ isomerization becomes important when the CH_3Br intramolecular modes are excited. Energy transfer between intermolecular and intramolecular modes is also inefficient for the $ClCH_3 \cdots Br^-$ complex, which does not immediately dissociate to $ClCH_3 + Br^-$ as predicted by RRKM theory but remains trapped for some time in the intramolecular complex formed by $Cl^- \cdots CH_3Br \rightarrow ClCH_3 \cdots Br^-$ isomerization. Thus, the dynamics of both $Cl^- \cdots CH_3Br$ and $ClCH_3 \cdots Br^-$ are interpreted in terms of intermolecular and intramolecular complexes, as depicted in Fig. 3.

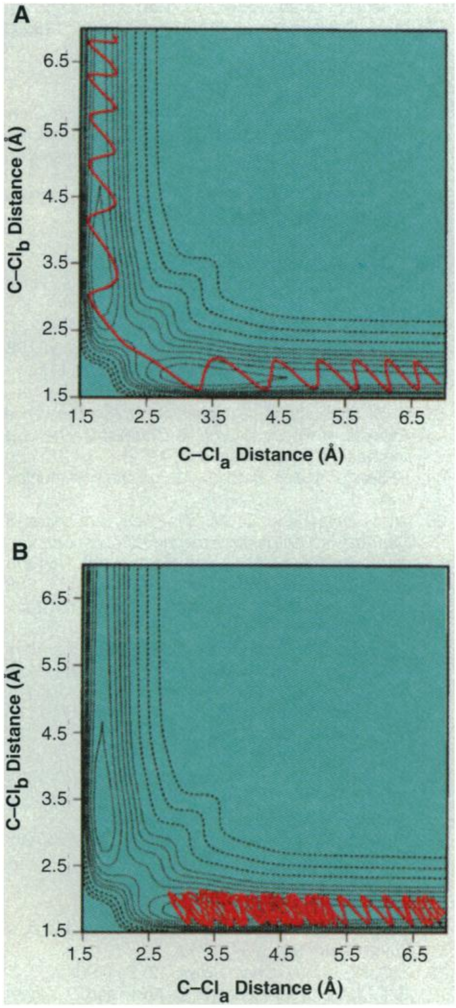

Fig. 2. Potential energy contour diagrams with (**A**) direct substitution and (**B**) complex-forming trajectories for the $Cl^- + CH_3Cl$ system. Each trajectory has a $Cl^- + CH_3Cl$ relative translational energy of 0.5 kcal/mol, no CH_3Cl rotational energy, and six quanta in the C–Cl stretch mode.

Weak coupling between the intermolecular and intramolecular modes of $ClCH_3 \cdots Br^-$ is inferred from experiment (43), in which the relative translational energies of the $ClCH_3 + Br^-$ products was measured. The experimental relative translational energies are lower than those predicted by OTS-PST (Fig. 4), which assumes a statistical distribution of vibrational, rotational, and translational energies at the orbiting transition state. The distribution of relative translational energy, determined from the trajectory simulation (62), is nearly identical to the experimental result. The trajectory simulations show that product energy is preferentially partitioned to $ClCH_3$ vibration.

Central Barrier Recrossing

The dynamical model described in Fig. 3 indicates that the trajectories may recross the central barrier several times if the $C_{\mathrm{intra,R}} \leftrightarrow C_{\mathrm{intra,P}}$ transition is faster than the transitions between the intermolecular and intramolecular complexes. For a S_N2 reaction such as $Cl^- + CH_3Cl$, for which TST assumes that crossing of the central barrier is rate determining, such recrossings would make TST an incomplete model for calculating the S_N2 rate constant. It would be necessary to correct the TST rate constant by a factor κ, which is the number of reactive trajectories divided by the number of central barrier crossings in the R → P direction; that is, $k_{S_N2} = \kappa\, k_{\mathrm{TST}}$ (TST assumes $\kappa = 1$).

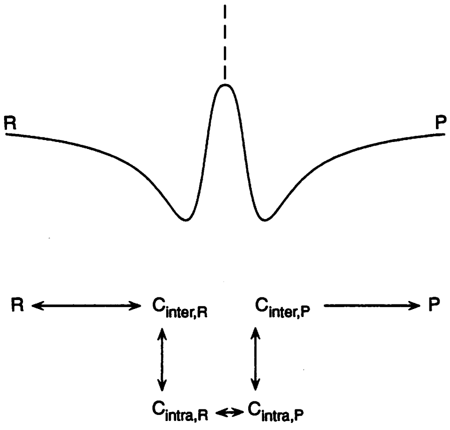

Fig. 3. Dynamical model for S_N2 nucleophilic substitution. The labels R and P denote the reactant and product sides of the central barrier, respectively.

The most direct way of calculating this recrossing factor is to initiate the trajectories at the central barrier and select their initial values of q_i and p_i according to a Boltzmann distribution (76, 77). TST predicts each trajectory that crosses the central barrier in the R → P direction forms products without central barrier recrossings. Trajectory calculations of this type, performed for the $Cl^- + CH_3Cl$ S_N2 reaction (60), give a κ factor less than unity, in the

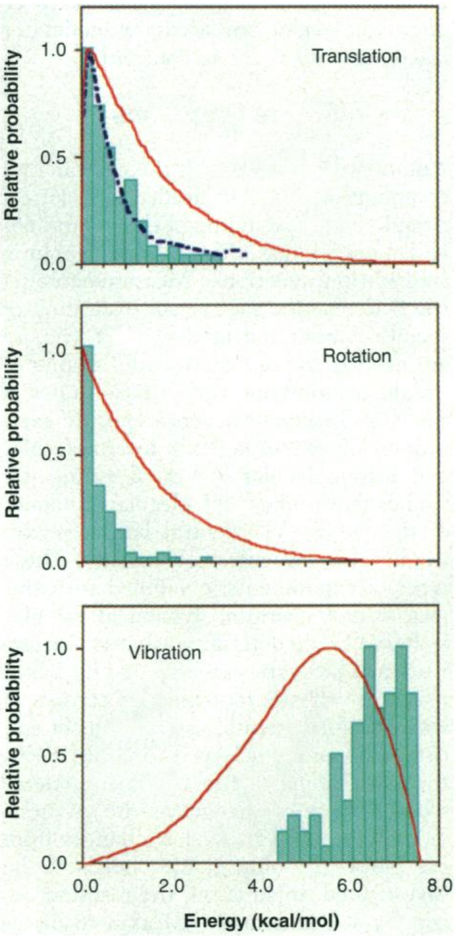

Fig. 4. Product energy distributions for the $Cl^- \cdots CH_3Br \rightarrow ClCH_3 + Br^-$ reaction: histogram, trajectory result (62); dashed line, experiment (43); and solid line, prediction of OTS-PST. The trajectory results (62) are scaled to match the experimental exothermicity.

range of 0.1 to 0.3. The uncertainty in κ arises from (i) long-time trapping of the trajectories near the central barrier so that the R and P asymptotic limits are not reached and (ii) uncertainty in the treatment of the zero-point energy for the barrier recrossing trajectories. Thus, the trajectories predict that both the $C_{\text{inter}} \leftrightarrow C_{\text{intra}}$ transitions and the $C_{\text{intra,R}} \leftrightarrow C_{\text{intra,P}}$ transitions affect the rate of $Cl^- + CH_3Cl$ S_N2 nucleophilic substitution.

If trapping in the ion-dipole complex must be incorporated into the statistical model, so that the S_N2 rate constant is given by Eq. 4, then it is more difficult to represent the effect of central barrier recrossings; correcting TST with the κ factor is not enough. The recrossings and presence of both intermolecular and intramolecular complexes are expected to affect the k_{as}, k_{isom}, and k_{dis} rate constants in Eq. 4. The value for k_{as} should be smaller than that of a capture model, and k_{isom} and k_{dis} should disagree with the predictions of RRKM theory. The Cl^- + CH_3Br system appears to behave in this manner (*62*), and more work needs to be done to develop an accurate model for calculating its S_N2 rate constant.

Future Directions

Additional experimental, theoretical, and computational work is needed to acquire a complete understanding of the microscopic dynamics of gas-phase S_N2 nucleophilic substitution reactions. Measurements of the S_N2 reaction rate versus excitation of specific vibrational modes of RY (Eq. 2) are needed, as are experimental studies of the dissociation and isomerization rates of the $X^-\cdots RY$ complex versus specific excitations of the complex's intermolecular and intramolecular modes. Experimental studies that probe the molecular dynamics of the $[X\cdots R\cdots Y]^-$ central barrier region would also be extremely useful. These types of experiments, combined with trajectory and quantum dynamical calculations, will help determine what characteristics and properties are required for a S_N2 reaction to make its dynamics consistent with the fundamental assumptions of statistical theories such as TST and RRKM theory. The manner in which the microscopic dynamics changes as the environment for the S_N2 reaction changes from gas phase to solution also needs to be investigated. In solution, the reaction occurs by a mechanism (*78*) akin to direct substitution in the gas phase without trapping in an ion-dipole complex (*79*). Finally, more accurate TST and RRKM calculations are needed, which include anharmonicity in the partition functions and densities of state for the RY reactant, $X^-\cdots RY$ complex, and $[X\cdots R\cdots Y]^-$ transition state, to facilitate comparisons between experiments and dynamical calculations and statistical theories.

REFERENCES AND NOTES

1. J. I. Steinfeld, J. S. Francisco, W. L. Hase, *Chemical Kinetics and Dynamics* (Prentice-Hall, Englewood Cliffs, NJ, 1989).
2. R. D. Levine and R. B. Bernstein, *Molecular Reaction Dynamics and Chemical Reactivity* (Oxford Univ. Press, New York, 1987).
3. W. L. Hase, Ed., *Intramolecular and Nonlinear Dynamics*, vol. 1. of *Advances in Classical Trajectory Methods* (JAI Press, Greenwich, CT, 1992).
4. T. Uzer, *Phys. Rep.* **199**, 73 (1991).
5. S. Glasstone, K. J. Laidler, H. Eyring, *The Theory of Rate Processes* (McGraw-Hill, New York, 1941).
6. R. A. Marcus and O. K. Rice, *J. Phys. Colloid. Chem.* **55**, 894 (1951); R. A. Marcus, *J. Chem. Phys.* **20**, 359 (1952).
7. J. Horiuti, *Bull. Chem. Soc. Jpn.* **13**, 210 (1938).
8. K. J . Laidler, *Theory of Chemical Reaction Rates* (McGraw-Hill, New York, 1969), p. 76.
9. W. L. Hase, *J. Chem. Phys.* **64**, 2442 (1976).
10. B. C. Garrett and D. G. Truhlar, *ibid.* **70**, 1593 (1979); D. G. Truhlar, A. D. Issacson, B. C. Garrett, in *Theory of Chemical Reaction Dynamics*, M. Baer, Ed. (CRC Press, Boca Raton, FL, 1985), vol. 4, pp. 65–137.
11. W. L. Hase, in *Modern Theoretical Chemistry*, W. H. Miller, Ed. (Plenum, New York, 1976), vol. 2, pp. 121–169.
12. D. L. Bunker and M. Pattengill, *J. Chem. Phys.* **48**, 772 (1968).
13. W. L. Hase, *Acc. Chem. Res.* **16**, 258 (1983).
14. D. M. Wardlaw and R. A. Marcus, *Adv. Chem. Phys.* **70**, 231 (1988).
15. P. Pechukas and J. C. Light, *J. Chem. Phys.* **42**, 3281 (1965); P. Pechukas, C. Rankin, J. C. Light, *ibid.* **44**, 796 (1966).
16. C. E. Klots, *J. Phys. Chem.* **75**, 1526 (1971); *Z. Naturforsch. A* **27**, 553 (1972); *J. Chem. Phys.* **64**, 4269 (1976).
17. M. Quack and J. Troe, *Ber. Bunsenges. Phys. Chem.* **78**, 240 (1974); *ibid.* **79**, 170 (1975).
18. W. J. Chesnavich and M. T. Bowers, *J. Chem. Phys.* **66**, 2306 (1977); in *Gas Phase Ion Chemistry*, M. T. Bowers, Ed. (Academic Press, New York, 1979), vol. 1, pp. 119–151.
19. R. A. Marcus, *J. Chem. Phys.* **85**, 5035 (1986).
20. A. H. Zewail and R. B. Bernstein, *Chem. Eng. News* **66**, 24 (7 November 1988).
21. A. H. Zewail, Ed., *Femtochemistry: Ultrafast Dynamics of the Chemical Bond* (World Scientific, London, 1994), vols. 1 and 2.
22. D. L. Bunker, *Sci. Am.* **211**, 100 (July 1964).
23. G. C. Lynch *et al.*, *J. Chem. Phys.* **94**, 7150 (1991).
24. D. C. Clary and J. Echave, in *Reactive Scattering*, vol. 2A of *Advances in Molecular Vibrations and Collision Dynamics*, J. M. Bowman, Ed. (JAI Press, Greenwich, CT, 1993), pp. 203–243.
25. R. T. Pack, E. A. Butcher, G. A. Parker, *J. Chem. Phys.* **99**, 9310 (1993).
26. U. Manthe, T. Seideman, W. H. Miller, *ibid.*, p. 10078.
27. D. L. Bunker, *Methods Comput. Phys.* **10**, 287 (1971).
28. L. M. Raff and D. L. Thompson, in *Theory of Chemical Reaction Dynamics*, M. Baer, Ed. (CRC Press, Boca Raton, FL, 1985), vol. 3, pp. 1–121.
29. H. Goldstein, *Classical Mechanics* (Addison-Wesley, London, 1950).
30. W. E. Farneth and J. I. Brauman, *J. Am. Chem. Soc.* **98**, 7891 (1976); W. N. Olmstead and J. I. Brauman, *ibid.* **99**, 4219 (1977).
31. M. J. Pellerite and J. I. Brauman, *ibid.* **105**, 2672 (1983).
32. J. A. Dodd and J. I. Brauman, *J. Phys. Chem.* **90**, 3559 (1986).
33. G. Caldwell, T. F. Magnera, P. Kebarle, *J. Am. Chem. Soc.* **106**, 959 (1984).
34. S. E. Barlow, J. M. Van Doren, V. M. Bierbaum, *ibid.* **110**, 7240 (1988).
35. T. Su, R. A. Morris, A. A. Viggiano, J. F. Paulson, *J. Phys. Chem.* **94**, 8426 (1990).
36. C. H. DePuy, S. Gronert, A. Mullin, V. M. Bierbaum, *J. Am. Chem. Soc.* **112**, 8650 (1990).
37. A. A. Viggiano *et al.*, *ibid.* **113**, 9404 (1991).
38. D. M. Cyr, L. A. Posey, G. A. Bishea, C.-C. Han, M. A. Johnson, *ibid.*, p. 9697.
39. A. A. Viggiano, R. A. Morris, J. S. Paschkewitz, J. F. Paulson, *ibid.* **114**, 10477 (1992).
40. B. D. Wladkowski, K. F. Lim, W. D. Allen, J. I. Brauman, *ibid.*, p. 9136; A. A. Viggiano *et al.*, *ibid.* **116**, 2213 (1994).
41. W. B. Knighton, J. A. Bognan, P. M. O'Connor, E. P. Grimsrud, *ibid.* **115**, 12079 (1993).
42. D. M. Cyr, M. G. Scarton, M. A. Johnson, *J. Chem. Phys.* **99**, 4869 (1993).
43. S. T. Graul and M. T. Bowers, *J. Am. Chem. Soc.* **113**, 9696 (1991); *ibid.* **116**, 3875 (1994).
44. C. D. Ritchie and G. A. Chappell, *ibid.* **92**, 1819 (1970).
45. A. Dedieu and A. Veillard, *Chem. Phys. Lett.* **5**, 328 (1970); *J. Am. Chem. Soc.* **94**, 6730 (1972).
46. H. B. Schlegel, K. Mislow, F. Bernardi, A. Bottoni, *Theor. Chim. Acta* **44**, 245 (1977).
47. S. Wolfe, D. J. Mitchell, H. B. Schlegel, *J. Am. Chem. Soc.* **103**, 7692 (1981).
48. S. S. Shaik, H. B. Schlegel, S. Wolfe, *J. Chem. Soc. Chem. Commun.* **1988**, 1322 (1988).
49. Z. Shi and R. J. Boyd, *J. Am. Chem. Soc.* **112**, 6789 (1990).
50. S. C. Tucker and D. G. Truhlar, *ibid.*, p. 3338.
51. R. Vetter and L. Zülicke, *ibid.*, p. 5136.
52. F. Jensen, *Chem. Phys. Lett.* **196**, 368 (1992).
53. M. V. Basilevsky and V. M. Ryaboy, *ibid.* **129**, 71 (1986).
54. V. M. Ryaboy, *ibid.* **159**, 371 (1989).
55. G. D. Billing, *Chem. Phys.* **159**, 109 (1992).
56. V. M. Ryaboy, in *Dynamics of Ion-Molecule Complexes*, vol. 2 of *Advances in Classical Trajectory Methods*, W. L. Hase, Ed. (JAI Press, Greenwich, CT, 1994), pp. 115–145.
57. S. R. Vande Linde and W. L. Hase, *J. Am. Chem. Soc.* **111**, 2349 (1989).
58. ______, *J. Phys. Chem.* **94**, 6148 (1990).
59. ______, *J. Chem. Phys.* **93**, 7962 (1990).
60. Y. J. Cho, S. R. Vande Linde, L. Zhu, W. L. Hase, *ibid.* **96**, 8275 (1992).
61. W. L. Hase and Y. J. Cho, *ibid.* **98**, 8626 (1993).
62. H. Wang, L. Zhu, W. L. Hase, *J. Phys. Chem.* **98**, 1608 (1994); H. Wang, G. H. Peslherbe, W. L. Hase, *J. Am. Chem. Soc.* **116**, 9644 (1994).
63. S. S. Shaik, H. B. Schlegel, S. Wolfe, *Theoretical Aspects of Physical Organic Chemistry: The S_N2 Mechanism* (Wiley, New York, 1992).
64. S. Seeger and P. Botschwina, private communication.
65. W. L. Hase and D. M. Wardlaw, *Advances in Gas-Phase Photochemistry and Kinetics: Bimolecular Collisions*, M. N. R. Ashfold and J. E. Baggott, Eds. (Royal Society, London, 1989), pp. 171–208.
66. W. J. Chesnavich, T. Su, M. T. Bowers, *J. Chem. Phys.* **72**, 2641 (1980).
67. T. Su and M. T. Bowers, in *Gas Phase Ion Chemistry*, M. T. Bowers, Ed. (Academic Press, New York, 1979), vol. 1, pp. 84–118.
68. T. Su and W. J. Chesnavich, *J. Chem. Phys.* **76**, 5183 (1982).
69. R. E. Miller, *Science* **240**, 447 (1988).
70. S. Chapman and D. L. Bunker, *J. Chem. Phys.* **62**, 2890 (1975).
71. S. H. Bauer, *Chem. Rev.* **78**, 147 (1978).
72. M. Kneba and J. Wolfrum, *Annu. Rev. Phys. Chem.* **31**, 47 (1980).
73. J. C. Polanyi, *Science* **236**, 680 (1987).
74. T. McMahon, private communication.
75. I. Benjamin, A. Liu, K. R. Wilson, R. D. Levine, *J. Phys. Chem.* **94**, 3937 (1990).
76. J. C. Keck, *Adv. Chem. Phys.* **13**, 85 (1967).
77. R. L. Jaffe, J. M. Henry, J. B. Anderson, *J. Chem. Phys.* **59**, 1128 (1973).
78. B. J. Gertner, R. M. Whitnell, K. R. Wilson, J. T. Hynes, *J. Am. Chem. Soc.* **113**, 74 (1991).
79. J. Chandrasekhar and W. L. Jorgensen, *ibid.* **107**, 2974 (1985).
80. I thank G. Peslherbe and H. Wang for preparing the figures and J. I. Brauman, H. B. Schlegel, and S. C. Tucker for helpful discussions.